

# Hypochlorite Ion Decomposition: Effects of Temperature, Ionic Strength, and Chloride Ion

Luke C. Adam and Gilbert Gordon\*

Department of Chemistry, Miami University, Oxford, Ohio 45056

Received January 7, 1998

The effects of pH, hypochlorite and chloride ion concentration, temperature, and ionic strength on the kinetics and mechanism of decomposition of concentrated hypochlorite ion and the formation of chlorate ion and oxygen in the pH 9–14 region has been investigated. In the absence of catalytic levels of transition-metal ions, the rate of chlorate ion formation is 8.7 times faster than the rate of oxygen formation for the concentration range of 0.7–3.0 M hypochlorite ion with various levels of chloride ion in 0.001–1.0 M OH<sup>-</sup> at 15–55 °C. Under these same conditions, the equation that describes the effect of temperature and ionic strength on the decomposition of OCl<sup>-</sup> is the following:  $\log k_2 = 0.149\mu + \log[2.083 \times 10^{10} T \exp(-1.018 \times 10^5/RT) \exp(-56.5/R)]$  where  $k_2$  has units of M<sup>-1</sup> sec<sup>-1</sup> and  $\mu$  is between 1 and 6 molar. Numerical simulation of the decomposition of OCl<sup>-</sup> was carried out while taking into account the effect of each of the above experimental variables. Evidence is presented suggesting chloride ion catalyzed decomposition of hypochlorite ion in the pH 9–10 region that is in addition to the contribution of chloride ion to the ionic strength.

## Introduction

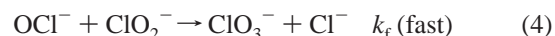
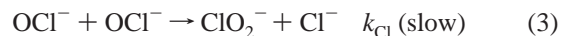
Hypochlorite ion, a commonly used oxidizing agent for the disinfection of drinking water,<sup>1</sup> is known<sup>2,3</sup> to decompose to form chlorate ion and oxygen. Chlorate ion, often present in drinking water<sup>4–8</sup> that has been treated with OCl<sup>-</sup>, may pose potential health<sup>9</sup> hazards. Chlorate ion is listed as a compound for which regulation<sup>10–12</sup> by the USEPA may be set by the year 2000. Thus, it is important to have a detailed understanding of the kinetics and mechanism of OCl<sup>-</sup> decomposition in order to minimize the formation of ClO<sub>3</sub><sup>-</sup>.

Hypochlorite ion decomposition in basic solution is a slow second-order process<sup>3</sup> in the 40–60 °C region with the following stoichiometry and rate law:



$$-d[\text{OCl}^-]/3dt = k_{\text{obs}}[\text{OCl}^-]^2 \quad (2)$$

The decomposition of OCl<sup>-</sup> involves chlorite ion (ClO<sub>2</sub><sup>-</sup>) as an intermediate<sup>13</sup> in the following generally accepted mechanism:



Because reaction 4 is the faster<sup>3</sup> step, the concentration of ClO<sub>2</sub><sup>-</sup> is relatively low.

Prior to 1950, commercial OCl<sup>-</sup> was known to contain transition-metal ions, including platinum, iridium, and rhodium, that were demonstrated<sup>14</sup> to be effective catalysts for the decomposition of OCl<sup>-</sup>. Although improvements in OCl<sup>-</sup> manufacture eliminated most platinum group metal ions, the decomposition may be catalyzed<sup>2,3</sup> by other transition-metal ions such as Ni(II), Cu(II), Mn(II), and Fe(III).

The formation of oxygen<sup>15</sup> from decomposing OCl<sup>-</sup> solutions is a very slow side reaction in solutions of pure OCl<sup>-</sup> and is a minor decomposition pathway:

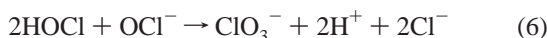


The reaction to form O<sub>2</sub> is catalyzed by the above transition-metal ion impurities. The rate constants of reactions 3–5 are affected not only by temperature but also by the ionic strength, ionic media present, and the presence<sup>15,16</sup> and intensity of UV light.

- (1) White, G. C. *Handbook of Chlorination*, 2nd ed.; Van Nostrand Reinhold Company Inc.: New York, 1986.
- (2) Lister, M. W. *Can. J. Chem.* **1952**, *30*, 879.
- (3) Lister, M. W. *Can. J. Chem.* **1956**, *34*, 479.
- (4) Gordon G. The Formation of Chlorate Ion in Drinking Water Treated with Free Available Chlorine. Presented to the D/DBP TAW in session at the Water Quality Technology Conference, (Orlando, FL, November 1991).
- (5) Bolyard, M.; Fair, P. S.; Hautman, D. P. *Environ. Sci. Technol.* **1992**, *26*, 1663.
- (6) Gordon, G.; Adam, L. C.; Bubnis, B. P.; Hoyt, B.; Gillette, S. J.; Wilczac, A. *J. Am. Water Works Assoc.* **1993**, *86*(9), 89.
- (7) Bolyard, M.; Fair, P. S.; Hautman, D. P. *J. Am. Water Works Assoc.*, **1993**, *85*(9), 81.
- (8) Gordon, G.; Adam, L. C.; Bubnis, B. P. *Minimizing Chlorate Ion Formation in Drinking Water When Hypochlorite Ion is the Chlorinating Agent*. AWWA Research Foundation, Denver, CO, Contract 833-92, 1994.
- (9) *Drinking Water and Health*; Boraks, J., Ed.; National Research Council, National Academy Press: Washington, DC, 1987; pp 99–111.
- (10) Regli, S. EPA Presentation to AWWA Technical Advisory Workgroup, November, 1990. Discussion of Strawman Rule for Disinfection Byproducts. Presented to EPA Science Advisory Board Drinking Water Committee, September, 1989.
- (11) Federal Register. *Priority List of Substances Which May Require Regulation Under the Safe Drinking Water Act*; EPA, 1991, 56:9:1470–1474.
- (12) EPA. *Safe Drinking Water Hotline*; 1997, 1 (800) 426-4791.
- (13) Adam, L. C.; Suzuki, K.; Fábíán, I.; Gordon, G. *Inorg. Chem.* **1992**, *31*, 3534.

- (14) Ayres, G. H.; Booth, M. H. *J. Am. Chem. Soc.* **1955**, *77*, 825–827.
- (15) Lister, M. W.; Petterson, R. C. *Can. J. Chem.* **1962**, *40*, 729.
- (16) *Sodium Hypochlorite Safety and Handling*, Pamphlet 96, 1st ed.; Chlorine Institute: Washington, DC, 1992; p 17.
- (17) Yokoyama, T.; Takayasu, O. *Kogyo Kagaku Zasshi* **1967**, *70*, 1619.
- (18) Chapin, R. M. *J. Am. Chem. Soc.* **1934**, *56*, 2211.

The decomposition of hypochlorous acid (HOCl) in the pH 5–9 region<sup>13,17,18</sup> proceeds according to the following reaction stoichiometry:



which can also be expressed as  $3\text{ClO}^- \rightarrow 2\text{Cl}^- + \text{ClO}_3^-$  when  $[\text{OCI}^-] > [\text{H}^+]$  or as  $3\text{HOCl} \rightarrow 2\text{Cl}^- + \text{ClO}_3^- + 3\text{H}^+$  when  $[\text{OCI}^-] \leq [\text{H}^+]$ .

The simplified rate law is

$$-d([\text{HOCl}] + [\text{OCI}^-])/3dt = k_{\text{obs}}[\text{HOCl}]^2[\text{OCI}^-] \quad (7)$$

The measured third-order rate constant<sup>13</sup> ( $k_{\text{obs}}$ ) is  $0.0125 \text{ M}^{-2} \text{ s}^{-1}$  at  $25^\circ \text{C}$ . The activation parameters<sup>13</sup> are  $\Delta H^\ddagger = 64.0 \pm 0.6 \text{ kJ/mol}$  and  $\Delta S^\ddagger = -67 \pm 2 \text{ J/mol K}$  in  $1.0 \text{ M NaClO}_4$ . As implied by eq 7 and demonstrated experimentally, the rate of decomposition reaches a maximum when the ratio of HOCl to  $\text{OCI}^-$  is equal to 2.0. Using an HOCl  $\text{p}K_{\text{a}}$  of 7.54 ( $25^\circ \text{C}$ ,  $\mu = 0$ ), the rate of decomposition has a maximum at pH 7.24 and decreases significantly at higher and lower pH values. As decomposition occurs in the pH 7.24–10 region, the  $\text{OCI}^-$  to HOCl ratio decreases, which decreases the pH of the solution and increases the rate of decomposition.

The primary objective of this work was to determine how the  $\text{OH}^-$ ,  $\text{OCI}^-$ , and  $\text{Cl}^-$  concentrations, temperature, and ionic strength affect the kinetics and mechanism of decomposition of concentrated  $\text{OCI}^-$  and the formation of  $\text{ClO}_3^-$  and  $\text{O}_2$  in the pH 9–14 region. Each of these experimental variables was studied in a series of decomposition experiments in which the change in concentration of  $\text{OCI}^-$ ,  $\text{ClO}_3^-$ ,  $\text{ClO}_2^-$ ,  $\text{OH}^-$ , and  $\text{CO}_3^{2-}$  was measured as a function of time.

## Experimental Section

**Reagents.** All solutions were prepared using high quality chlorine demand free deionized triply distilled water from a Barnstead/NANOpure water purification system. Chlorite ion standards were prepared from triply recrystallized<sup>19,20</sup> sodium chlorite with a purity of 99.64%. All other reagents were prepared from ACS reagent grade chemicals. Concentrated sodium hypochlorite was prepared by means of the Cady<sup>21</sup> method. Commercially prepared  $\text{OCI}^-$  containing low levels of transition-metal ions and nearly equivalent  $\text{OCI}^-$  and  $\text{Cl}^-$  concentrations was also used in some experiments.

**Methodology.** Sodium hypochlorite solutions were analyzed for  $\text{OCI}^-$ ,  $\text{ClO}_2^-$ ,  $\text{ClO}_3^-$ ,  $\text{OH}^-$ ,  $\text{CO}_3^{2-}$ , and  $\text{Cl}^-$ . The concentrations of  $\text{OCI}^-$ ,  $\text{OH}^-$ , and  $\text{CO}_3^{2-}$  were determined by potentiometric titration using a VIT 90 Video Titrator equipped with a P101 platinum K401 SCE electrode pair and GK2401B combination pH electrode (Radiometer, Copenhagen, Denmark). The concentrations of NaOH and  $\text{Na}_2\text{CO}_3$  in the sodium hypochlorite were measured by potentiometric inflection point titration after removal of  $\text{OCI}^-$  using 0.6%  $\text{H}_2\text{O}_2$ . The measurement of  $\text{Cl}^-$  was carried out using a  $\text{Cl}^-$  selective electrode connected to a PHM 64 pH meter from Radiometer. Samples of  $\text{OCI}^-$  were prepared for measurement by the addition of ethylenediamine<sup>5,7</sup> (en) to remove  $\text{OCI}^-$ . Sodium hypochlorite solutions were analyzed directly for  $\text{ClO}_2^-$  and  $\text{ClO}_3^-$  by ion chromatography (IC) using a Dionex DX-100, Dionex Corp., Sunnyvale, CA. The chromatographic conditions<sup>6</sup> used have been reported. The  $\text{OCI}^-$  was removed by the addition of 0.5 mL of 1 M en per 100 mL of sample.

A variation of the iodometric method<sup>22,23</sup> was used to measure the sum of  $\text{OCI}^- + \text{ClO}_2^-$  at pH 1.3. The  $\text{ClO}_2^-$  concentration was determined by ion chromatography, and the  $\text{OCI}^-$  concentration was

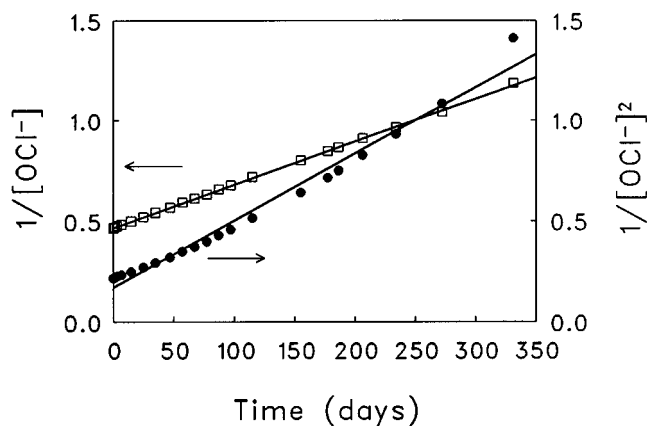


**Figure 1.** Second- and third-order plots of decomposing  $\text{OCI}^-$  with  $[\text{OCI}^-]_0 = 2.13 \text{ M}$ ,  $[\text{OH}^-] = 0.165 \text{ M}$ ,  $[\text{Cl}^-] = 0.158 \text{ M}$ , and  $\mu = 2.52 \text{ M}$  at  $25^\circ \text{C}$ .

calculated by difference. In some cases,  $\text{OCI}^-$  was titrated<sup>4,25</sup> directly using standard  $\text{Na}_2\text{SO}_3$  for method comparison.

The analysis of Fe, Ni, and Cu in  $\text{OCI}^-$  solutions was carried out using a Perkin-Elmer 1100B atomic absorption spectrophotometer. Potential matrix ion interferences were avoided by the dropwise addition of 15% v/v  $\text{H}_2\text{O}_2$  to an aliquot of  $\text{OCI}^-$  until the evolution of  $\text{O}_2$  was no longer evident. The solution was acidified to pH 1 with 2 M HCl and boiled to remove  $\text{H}_2\text{O}_2$  and  $\text{O}_2$ . The solution contained the transition-metal ions in 0.5–1.5 M NaCl. The sample metal ions were complexed,<sup>26</sup> extracted into 20 mL of MIBK, and analyzed. Standards in the 0.05–2 mg/L range of each transition-metal ion of interest were prepared in 1 M NaCl and extracted in the same manner as the samples.

The laboratory-prepared  $\text{OCI}^-$  solutions were analyzed for  $\text{Hg}^{2+}$  because  $\text{HgO}$  was used in the synthesis of  $\text{OCI}^-$ . The  $\text{OCI}^-$  sample was acidified, and  $\text{N}_2$  was bubbled through the sample to displace  $\text{Cl}_2$ . The sample was analyzed by the dithizone method.<sup>22</sup>

**Decomposition Experiments.** The experiments were carried out with an initial  $\text{OCI}^-$  concentration between 0.7 and 3 M  $\text{OCI}^-$ . All results refer to laboratory-prepared  $\text{OCI}^-$  unless specifically stated otherwise. Hypochlorite ion solutions were placed in 8.5 mL borosilicate vials with Teflon-lined caps and placed in water baths ( $\pm 0.05^\circ \text{C}$ ) in the dark.

## Results and Discussion

**Reaction Order.** Figure 1 shows representative second-order and third-order plots of 2.13 M  $\text{OCI}^-$  decomposition with an initial  $\text{OH}^-$  concentration of 0.165 M at  $25^\circ \text{C}$ . The plot of  $1/[\text{OCI}^-]$  vs time is linear throughout the experiment ( $\sigma \leq 0.0037$ ), whereas the  $1/[\text{OCI}^-]^2$  plot is increasingly nonlinear as the % decomposition increases, demonstrating that the decomposition is second-order in  $\text{OCI}^-$ . This second-order reaction behavior occurred for both laboratory-prepared and commercially produced  $\text{OCI}^-$ .

These results are consistent with that reported by Lister.<sup>3</sup> The second-order process is in agreement with the proposed change

(22) *Standard Methods for the Examination of Water and Wastewater*, 16th ed.; Cleseri, L. S., Greenberg, A. E., Trussell, R. R., Eds.; American Public Health Assoc.: Washington, DC, 1989; pp 232–234, 298–300.

(23) Gordon, G.; Cooper, W. J.; Rice, R. G.; Pacey, G. E. *Disinfectant Residual Measurement Methods: Second Ed.*; AWWA Research Foundation: Denver, CO, 1992; pp 9–10, 39–41, 53–55, 150–151.

(24) Suzuki, K.; Gordon, G. *Anal. Chem.* **1978**, *50*, 1596.

(25) Adam, L. C.; Gordon, G. *Anal. Chem.* **1995**, *34*, 535.

(26) Van Loon, J. C. *Analytical Atomic Absorption Spectroscopy: Selected Methods*, Academic Press: New York, NY, 1980, pp 80–81.

(27) *SCIENTIST: Mathematical Modeling Using Differential and Nonlinear Equations*; MicroMath Scientific Software, P.O. Box 21550 Salt Lake City, UT 84121, 1992.

(19) Nagypál, I.; Peintler, G.; Epstein, I. R. *J. Phys. Chem.* **1990**, *94*, 2954.

(20) Fábrián, I.; Gordon, G. *Inorg. Chem.* **1991**, *30*, 3785.

(21) Cady, G. H. *Inorganic Synthesis*; Moeller, T., Ed.; McGraw-Hill Company: New York, 1957; pp 156–165.

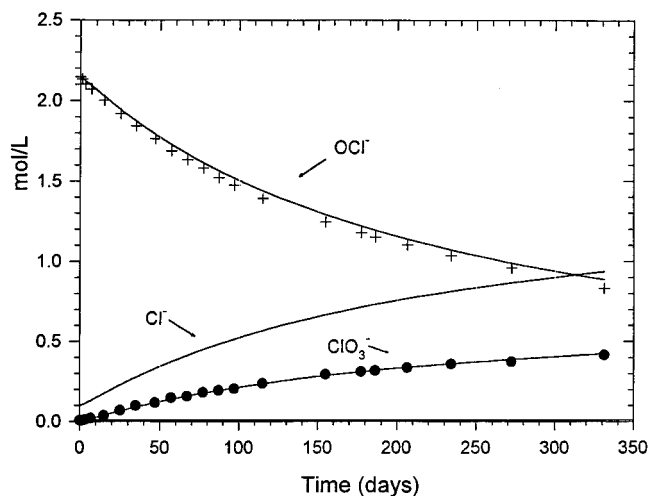


**Figure 2.** Measured and simulated decomposition of 2.15 M  $\text{OCl}^-$  at 25 °C with  $[\text{OH}^-] = 0.100 \text{ M}$ ,  $k_{\text{Cl}} = 7.70 \times 10^{-9} \text{ M}^{-1} \text{ s}^{-1}$ ,  $k_{\text{r}} = 1.54 \times 10^{-6} \text{ M}^{-1} \text{ s}^{-1}$ , and  $k_{\text{ox}} = 8.95 \times 10^{-10} \text{ M}^{-1} \text{ s}^{-1}$ .

in mechanism when compared to the third-order decomposition<sup>13</sup> that dominates in the pH 5–9 region.

A commercially available software package<sup>27</sup> was used for numerical simulation based on the EPISODE<sup>28</sup> integrator and least-squares data fitting using the Powell<sup>29</sup> algorithm. Numerical simulation was used to calculate the concentration of each species as a function of time to test the proposed mechanism and rate constants. Simulation results for the decomposition of 2.15 M  $\text{OCl}^-$  at pH 13 are shown in Figure 2. The lines correspond to simulated concentrations, and the symbols are experimental points. The simulated  $\text{OCl}^-$  and  $\text{ClO}_3^-$  concentrations agree with the measured concentrations to within 3%. The measured and fitted values of  $k_{\text{Cl}}$  (eq 3) are  $7.70 \times 10^{-9}$  and  $7.96 \pm 0.05 \times 10^{-9} \text{ M}^{-1} \text{ s}^{-1}$ , respectively. The simulated production of  $\text{O}_2$  and will be discussed later.

**Ionic Strength and Temperature.** Hypochlorite ion decomposition experiments were carried out with 2.13 and 3.07 M  $\text{OCl}^-$  at four NaCl concentrations ranging from 0.1–2.6 M. Each experiment was carried out at 25, 35, 45, and 55 °C for a total of 32 experiments. Additional experiments were carried out with commercial  $\text{OCl}^-$  solutions ranging from 0.6–2.8 M. Each of the commercial  $\text{OCl}^-$  decomposition experiments was carried out for 90 days at 15, 25, 35, 45, and 55 °C for a total of 60 additional experiments. The initial anion concentrations and the ionic strengths are given in Table 1 for all of the  $\text{OCl}^-$  solutions used.

The 2.164 and 2.974 M  $\text{OCl}^-$  solutions from Table 1 have similar ionic strengths, 4.830 and 4.913. The second-order plots of these solutions were linear, and the measured rate constants are compared in Table 2. The rate constants agree with an average error of 1%. The data in Table 2 show that  $\text{OCl}^-$  solutions with different  $\text{OCl}^-$  concentrations but similar ionic strengths have similar second-order rate constants. These results demonstrate that the NaCl added is contributing to the ionic strength and  $\text{Cl}^-$  is not involved mechanistically in 0.1 M  $\text{OH}^-$ . Second-order plots were linear for all 92 ionic strength–

**Table 1.** Initial Concentration of Each Anion Present and the Ionic Strengths for Each  $\text{OCl}^-$  Solution Used at Each Temperature

$[\text{OCl}^-]$ (M)	density (g/mL)	$[\text{Cl}^-]$ (M)	$[\text{OH}^-]$ (M)	$[\text{ClO}_3^-]$ (M)	$[\text{CO}_3^{2-}]$ (M)	$[\text{ClO}_2^-]$ (M)	$\mu$ (M)
Lab-Prepared $\text{OCl}^-$							
2.127	1.113	0.158	0.165	0.022	0.016	<LOD <sup>a</sup>	2.521
2.109	1.141	0.855	0.169	0.022	0.012	<LOD	3.190
2.117	1.169	1.514	0.168	0.022	0.011	<LOD	3.855
2.164	1.209	2.439	0.171	0.022	0.011	<LOD	4.830
3.065	1.154	0.264	0.120	0.036	0.011	0.001	3.520
3.026	1.182	0.959	0.122	0.036	0.011	0.001	4.176
2.974	1.213	1.754	0.121	0.034	0.010	0.001	4.913
2.969	1.247	2.581	0.114	0.034	0.010	0.001	5.729
Commercial $\text{OCl}^-$							
2.801	1.250	2.910	0.113	0.014	0.009	0.002	5.867
2.292	1.207	2.381	0.092	0.011	0.007	0.002	4.799
1.779	1.166	1.848	0.072	0.009	0.006	0.001	3.727
1.250	1.118	1.299	0.050	0.006	0.004	0.001	2.618
0.714	1.069	0.742	0.029	0.004	0.002	0.001	1.492
1.537	1.149	1.610	0.125	0.012	0.011	0.005	3.322
1.066	1.104	1.117	0.087	0.008	0.008	0.003	2.305
0.578	1.055	0.605	0.047	0.005	0.004	0.002	1.249
2.065	1.194	2.270	0.072	0.040	0.011	0.006	4.486
1.781	1.170	1.958	0.062	0.034	0.009	0.005	3.867
1.250	1.116	1.374	0.044	0.024	0.007	0.004	2.717
0.734	1.067	0.807	0.026	0.014	0.004	0.002	1.595

<sup>a</sup> LOD for  $[\text{ClO}_2^-] = 0.001 \text{ M}$ .

**Table 2.** Measured Second-Order Rate Constants for  $\text{OCl}^-$  Decomposition at Similar Ionic Strengths<sup>a</sup>

$T, ^\circ\text{C}$	$k_2$			% error <sup>b</sup>
	A	B	average	
25	5.88	5.82	5.86	1.0
35	21.5	21.2	21.3	1.5
45	76.4	76.4	76.4	0.0
55	235	231	233	1.4

<sup>a</sup> Conditions: (A)  $[\text{OH}^-] = 0.171$ ,  $[\text{OCl}^-] = 2.164$ ,  $\mu = 4.830$ ; (B)  $[\text{OH}^-] = 0.121$ ,  $[\text{OCl}^-] = 2.974$ ,  $\mu = 4.913$ . Units for  $k_2$  are  $\text{M}^{-1} \text{ s}^{-1} \times 10^8$ . <sup>b</sup>  $(\Delta k_2 / \text{average } k_2) \times 100$ .

**Table 3.** Measured Second-Order Rate Constants for  $\text{OCl}^-$  Decomposition at the Temperatures and Ionic Strengths Given<sup>a</sup>

$T, ^\circ\text{C}$	$\sim 0.17 \text{ M OH}^-, \sim 2.1 \text{ M OCl}^-$		$\sim 0.12 \text{ M OH}^-, \sim 3.0 \text{ M OCl}^-$	
	$\mu$	$k_2$	$\mu$	$k_2$
25	2.521	2.49	3.520	3.70
25	3.190	3.18	4.176	4.58
25	3.855	4.19	4.913	5.82
25	4.83	5.88	5.729	7.67
35	2.521	9.25	3.520	13.30
35	3.190	11.97	4.176	16.60
35	3.855	15.42	4.913	21.16
35	4.830	21.47	5.729	27.25
45	2.521	32.75	3.520	48.44
45	3.190	42.42	4.176	62.15
45	3.855	55.34	4.913	76.39
45	4.830	76.38	5.729	100.2
55	2.521	104.1	3.520	148.5
55	3.190	130.1	4.176	185.3
55	3.855	168.4	4.913	231.4
55	4.830	234.6	5.729	304.8

<sup>a</sup>  $k_2$  has three significant figures, but four have been presented in some cases to eliminate rounding errors in continuing data analysis. Units for  $k_2$  are  $\text{M}^{-1} \text{ s}^{-1} \times 10^8$ .

temperature experiments, with  $\sigma \leq 0.005$ . The measured second-order rate constants are given in Tables 3 and 4.

Each  $\text{OCl}^-$  concentration studied had a different ionic strength. Using  $k_2$  as the measured second-order rate constant

(28) Byrne, G.; Hindmarsh, A. EPISODE: An Experimental Package for the Integration of Systems of Ordinary Differential Equations with Banded Jacobians. Lawrence Livermore National Laboratory report, UCID-30132, Livermore CA, April, 1976.

(29) Powell, M. J. D. A FORTRAN Subroutine for Solving Systems of Nonlinear Algebraic Equations. *Numerical Methods for Nonlinear Algebraic Equations*; Robinowitz, P., Ed.; Gordon and Breach Scientific Publishers: New York, 1970; Chapter 7.

**Table 4.** Rate Constants for Commercial  $\text{OCl}^-$  Decomposition<sup>a</sup>

$T, ^\circ\text{C}$	$k_2$				
	$\mu = 5.867$	$\mu = 4.799$	$\mu = 3.727$	$\mu = 2.618$	$\mu = 1.492$
55	289	219	160	114	75.8
45	93.4	67.9	50.8	35.0	22.3
35	26.7	19.7	14.1	9.76	6.31
25	7.33	5.42	3.73	2.53	1.83
15	1.91	1.33	0.93	0.61	0.35
			$\mu = 3.322$	$\mu = 2.305$	$\mu = 1.249$
55			152	104	65.9
45			44.0	31.6	20.6
35			12.3	8.52	5.79
25			3.34	2.28	1.44
15			0.82	0.52	0.30
	$\mu = 4.486$	$\mu = 3.867$	$\mu = 2.717$	$\mu = 1.595$	
55	198	164	112	89.0	
45	64.1	54.2	36.3	24.9	
35	17.8	14.7	10.0	6.45	
25	4.84	3.96	2.59	1.63	
15	1.19	0.97	0.65	0.35	

<sup>a</sup>See Table 1 for individual ion concentrations. Units for  $k_2$  are  $\text{M}^{-1} \text{s}^{-1} \times 10^8$ .

for the decomposition of  $\text{OCl}^-$ , an empirical<sup>30</sup> relationship between the rate constant and the ionic strength ( $\mu$ ) has the following form:

$$\log k_2 = b\mu + C \quad (8)$$

where  $b$  and  $C$  are experimentally determined coefficients.

For the data in Tables 3 and 4, plots of  $\log k_2$  vs  $\mu$  are linear ( $\sigma \leq 0.014$ ) and  $b$  is 0.137, 0.147, 0.149, 0.155, and 0.155 for each plot at 55, 45, 35, 25, and 15 °C, respectively. The average value for  $b$  is  $0.149 \pm 0.005$ . The intercept ( $C$ ) for each plot is  $-6.31, -6.84, -7.41, -8.00,$  and  $-8.61$  at 55, 45, 35, 25, and 15 °C, respectively.

An Eyring<sup>33</sup> plot of the data using the intercepts is linear ( $\sigma \leq 0.019$ ). Combining eq 8 and the Eyring eq, the effect of ionic strength and temperature can be quantitatively described for 0.7–3.0 M  $\text{OCl}^-$  from 15–55 °C where  $k_2$  has units of  $\text{M}^{-1} \text{sec}^{-1}$ :

$$\log k_2 = 0.149\mu + \log[2.083 \times 10^{10} T \exp(-1.018 \times 10^5/RT) \exp(-56.5/R)] \quad (9)$$

Using eq 9, calculated values of  $k_2$  can be compared with measured  $k_2$  from various sources of  $\text{OCl}^-$ . The calculated rate constants have an average error of <5%. Using the values for the  $b$  term from each individual temperature produces calculated  $k_2$  values with an average error of 2%. The thermodynamic parameters of activation at various ionic strengths within the range of ionic strength used in this study are:

$\mu$ (mol/L) =	1	2	3	4	5	6
$\Delta H^\ddagger$ (kJ/mol) =	101.0	100.2	99.4	98.6	97.9	97.1
$\Delta S^\ddagger$ (J/mol °K) =	-56.2	-55.9	-55.6	-55.3	-55.1	-54.8

**Effect of Hydroxide Ion Concentration.** The concentration of  $\text{OCl}^-$ ,  $\text{ClO}_3^-$ ,  $\text{ClO}_2^-$ , and  $\text{OH}^-$  measured as a function of

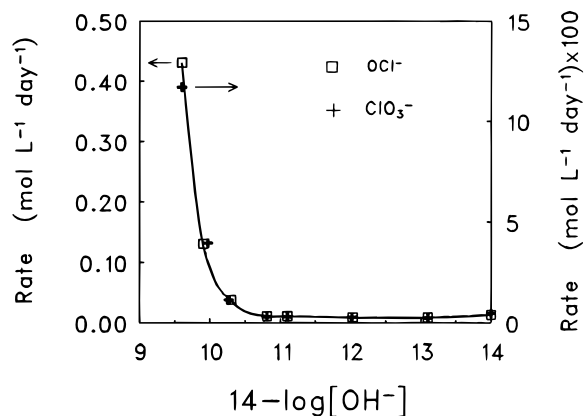


**Figure 3.** Initial rate of (10%)  $\text{OCl}^-$  decomposition and  $\text{ClO}_3^-$  formation as a function of  $[\text{OH}^-]$  with  $[\text{OCl}^-]_0 = 2.15 \text{ M}$  at 25 °C.

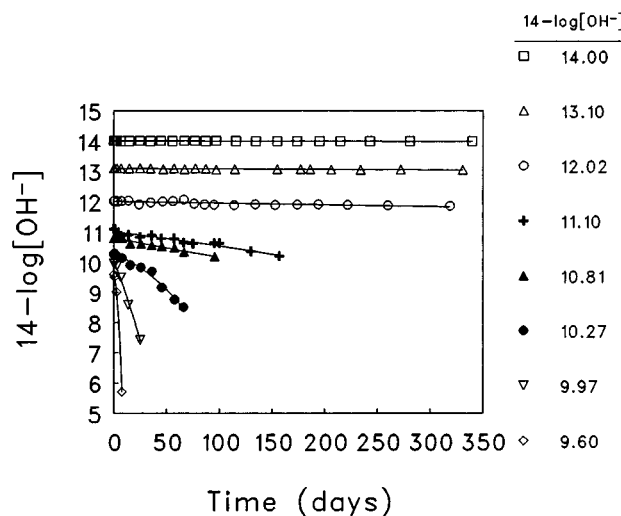


**Figure 4.** The pH of  $\text{OCl}^-$  decomposition as a function of time with  $[\text{OCl}^-]_0 = 2.15 \text{ M}$  at 25 °C.

time and the chlorine mass balance determined via eqs 3 and 4 is available as supporting material for eight experiments with  $[\text{OH}^-]$  between  $3.98 \times 10^{-5}$  and 1.00 M at 25 °C with an initial concentration of 2.15 M  $\text{OCl}^-$ . Figure 3 demonstrates the effect of  $\text{OH}^-$  concentration on the initial rate of  $\text{OCl}^-$  decomposition and  $\text{ClO}_3^-$  formation for these experiments. The decomposition has a minimum in the 0.001–0.1 M  $\text{OH}^-$  region. The presence of 1.0 M NaOH increases the initial rate of  $\text{OCl}^-$  decomposition by a factor of 1.5 compared to the presence of 0.01 M  $\text{OH}^-$ . This rate increase is due to an increase in the ionic strength as predicted by eq 8. At 0.00125 M  $\text{OH}^-$ , the rate of decomposition increases by a factor of 1.2 and increases dramatically below an  $\text{OH}^-$  concentration of  $3 \times 10^{-4} \text{ M}$ . Even though at this  $\text{OH}^-$  concentration the  $\text{HOCl}$  concentration is only  $1/1000$  of the  $\text{OCl}^-$  concentration, the mechanism of decomposition proposed in the pH 5–9 region is still the dominant pathway of  $\text{OCl}^-$  decomposition in  $3 \times 10^{-4} \text{ M OH}^-$ .

The  $\text{OCl}^-$  decomposition mechanism which dominates in the pH 5–9 region produces acid, as demonstrated in Figure 4 for eight experiments where  $[\text{OH}^-]$  is plotted as a function of time. Below an initial  $\text{OH}^-$  concentration of 0.01 M, the  $\text{OH}^-$  concentration of the  $\text{OCl}^-$  solutions decreases with time. Even though the initial rate of decomposition is at a minimum in the  $[\text{OH}^-] = 0.001\text{--}0.1 \text{ M}$  region,  $\text{OCl}^-$  solutions with an  $[\text{OH}^-]$  concentration below 0.01 M will slowly decrease in  $[\text{OH}^-]$

(30) Derivable equations such as the Davies (refs 31 and 32) equation are not applicable to the kinetic data because of the high ionic strengths (1–6M).

(31) Espenson, J. H. *Chemical Kinetics and Reaction Mechanisms*; McGraw-Hill Book Company, **1981**, 170, pp.

(32) Levine, I. N. *Physical Chemistry*, 3rd ed.; McGraw-Hill: New York, 1988; pp 851.

(33) Katakis, D.; Gordon, G. *Mechanisms of Inorganic Reactions*, Wiley-Interscience: New York, 1987; p 59.



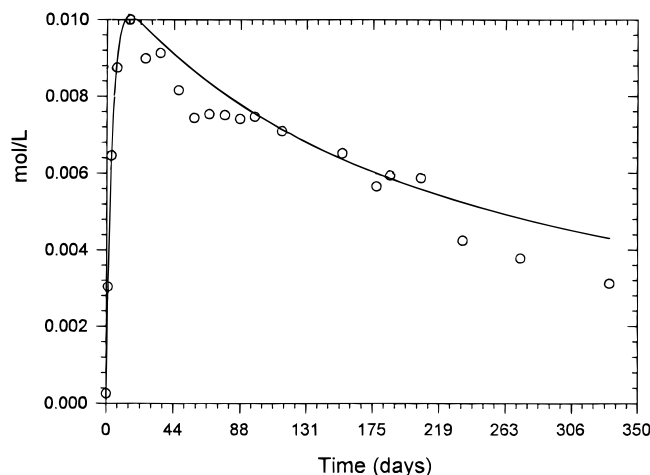


**Figure 5.** Measured and simulated  $\text{ClO}_2^-$  concentration with same conditions as Figure 2.

concentration, and the rate of decomposition increases significantly when the  $[\text{OH}^-]$  concentration drops below  $3 \times 10^{-4}$  M.

The slow rate of  $\text{OCl}^-$  decomposition above an  $\text{OH}^-$  concentration of  $3 \times 10^{-4}$  M as compared to that in the pH 5–9 region is consistent with a change in the mechanism of  $\text{OCl}^-$  decomposition. This change in mechanism is also supported by the fact that  $\text{ClO}_2^-$  is formed at measurable levels ( $\geq 2 \times 10^{-4}$  M) above an  $\text{OH}^-$  concentration of 0.001 M. The measured and simulated  $\text{ClO}_2^-$  concentrations for 2.15 M  $\text{OCl}^-$  in 0.126 M  $\text{OH}^-$  are shown in Figure 5. This simulation correctly predicts the rapid buildup of 0.01 M  $\text{ClO}_2^-$  and the subsequent slower decrease of  $\text{ClO}_2^-$  over time. The measured and fitted values for  $k_f$  (eq 4) are  $1.54 \times 10^{-6}$  and  $1.93 \pm 0.27 \times 10^{-6} \text{ M}^{-1} \text{ s}^{-1}$ , respectively.

In the pH 5–9 region, measurable<sup>13</sup>  $\text{ClO}_2^-$  is not present. Above an  $\text{OH}^-$  concentration of 0.01 M, the  $\text{ClO}_2^-$  level nominally approaches 0.5% of the  $\text{OCl}^-$  concentration at 25 °C. Chlorite ion is a relatively low concentration intermediate for  $\text{OH}^-$  concentrations  $> 0.001$  M. The  $\text{ClO}_2^-$  concentration quickly reaches a maximum and slowly decreases. At the point in time when  $[\text{ClO}_2^-]$  is at a maximum, the rate of  $\text{ClO}_2^-$  formation is equivalent to the rate of  $\text{ClO}_2^-$  loss and the corresponding terms in the derivative expression for  $\text{ClO}_2^-$  are equal:

$$k_{\text{Cl}}[\text{OCl}^-]^2 = k_f[\text{OCl}^-][\text{ClO}_2^-] \quad (10)$$

By rearranging this eq and using the concentrations at the time of maximum  $\text{ClO}_2^-$  formation, the ratio of  $k_f$  to  $k_{\text{Cl}}$  is estimated to be  $2 \times 10^2$  for the data set in Figure 5.

It should be noted that  $\text{OCl}^-$  decomposition data in 0.1 M  $\text{OH}^-$  with borate ion<sup>13</sup> at 90 °C shows that  $\text{ClO}_2^-$  can be formed in a concentration as high as 4.4% of the  $\text{OCl}^-$  concentration. Thus, the effect of temperature and matrix composition seem to be very important factors and may cause changes in the mechanism of  $\text{OCl}^-$  decomposition.

The individual decomposition mechanisms that dominate in the pH 5–9 region and above pH 11 were combined and applied to the numerical integration method. All following data simulations are produced using *both* decomposition mechanisms combined.

The simulated  $\text{OCl}^-$  and  $\text{ClO}_3^-$  concentrations obtained for 2.15 M  $\text{OCl}^-$  at initial pH values between 10.81 and 14.00 at 25 °C are in good agreement ( $\pm 5\%$ ) with the measured data

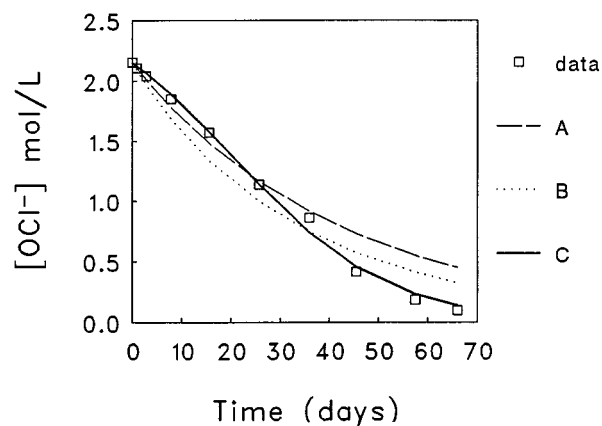
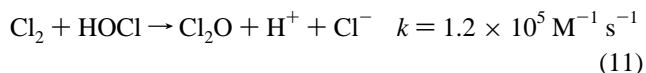


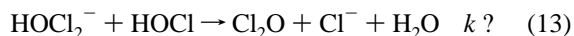
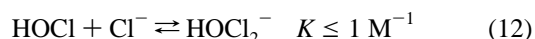
**Figure 6.** Simulation results obtained for 2.15 M  $\text{OCl}^-$  at an initial pH of 10.27 using  $k_{\text{Cl}} = 7.70 \times 10^{-9} \text{ M}^{-1} \text{ s}^{-1}$ ,  $k_f = 1.54 \times 10^{-6} \text{ M}^{-1} \text{ s}^{-1}$ , and  $k_{\text{Ox}} = 8.95 \times 10^{-10} \text{ M}^{-1} \text{ s}^{-1}$  using (A) no additional mechanistic steps, (B) a rate constant of  $1.2 \times 10^5 \text{ M}^{-1} \text{ s}^{-1}$  for eq 11, (C)  $K = 0.001$  and  $k = 1.3 \times 10^3 \text{ M}^{-1} \text{ s}^{-1}$  for eqs 12 and 13 and  $K_a = 7.94 \times 10^{-8}$ .

using  $k_{\text{Cl}} = 7.70 \times 10^{-9} \text{ M}^{-1} \text{ s}^{-1}$ ,  $k_f = 1.54 \times 10^{-6} \text{ M}^{-1} \text{ s}^{-1}$ , and  $k_{\text{Ox}} = 8.95 \times 10^{-10} \text{ M}^{-1} \text{ s}^{-1}$ . Figure 6 (simulation A) shows the result of the simulation of the pH<sub>0</sub> 10.27 data using both mechanisms of  $\text{OCl}^-$  decomposition. After 65% decomposition, there is an obvious discontinuity in the data that the simulation does not demonstrate. All laboratory and commercial  $\text{OCl}^-$  decomposition data in the initial pH range of 9–10.5 demonstrate the discontinuity which cannot be reproduced through simulation of the data using both mechanisms. The following equation<sup>34</sup> was added to the mechanism and used to produce simulation B:



The addition of this equation does not produce a significant improvement in the data simulation. Increasing the rate constant of eq 11 from  $1.2 \times 10^5 \text{ M}^{-1} \text{ s}^{-1}$  to the diffusion-controlled limit and repeating the simulation with various values for  $K_a$  (between  $1 \times 10^{-7}$  and  $3 \times 10^{-8}$ ) did not improve the simulation results.

The following equations<sup>35</sup> were added to the mechanism and produced simulation C in Figure 6:



The simulation result obtained using  $K = 0.001$  (eq 12),  $k = 1.3 \times 10^3 \text{ M}^{-1} \text{ s}^{-1}$  (eq 13), and  $K_a = 7.94 \times 10^{-8}$  M represents a significantly improved fit of the measured data ( $\sigma = 0.38$ , 0.25, and 0.02 for lines A, B, and C, respectively). Thus, the simulation result suggests that  $\text{Cl}^-$  catalyzed decomposition may be occurring in this pH region.

In summary, eqs 3–5 provide an accurate description of the  $\text{OCl}^-$  decomposition in the pH 11–14 region. The inclusion of the decomposition mechanism<sup>13</sup> that dominates in the pH 5–9 region and eqs 12 and 13 describes the decomposition of  $\text{OCl}^-$  throughout the pH 5–14 region.

(34) Beach, M. W.; Margerum, D. W. *Inorg. Chem.* **1990**, *29*, 1225.

(35) Espenson, L. H. *Investigations of Rates and Mechanisms of Reactions*; John Wiley and Sons: New York, 1986; Vol. 6, Part 1, pp 552.

**Table 5.** Rate Constants for  $\text{OCl}^-$  Decomposition at Various  $\text{OH}^-$  Concentrations<sup>a</sup>

$14 - \log [\text{OH}^-]$	slope	$k_{\text{Cl}}/k_{\text{Ox}}$	$3k_{\text{Cl}} + 2k_{\text{Ox}}$	$k_{\text{Cl}}$	$k_{\text{Ox}}$
Lab-Prepared $\text{OCl}^-$					
14.00	3.25	8.0	3.76	1.16	0.145
13.10	3.10	20	2.50	0.806	0.040
12.02	3.12	16.7	2.44	0.783	0.047
11.10	3.18	11.1	3.29	1.03	0.093
10.81	3.18	11.1	3.50	1.10	0.099
10.27	3.15	13.3	17.8	5.66	0.424
9.97	3.26	7.7	64.7	19.8	2.58
9.60	3.15	13.3	139	44.1	3.31
Commercial $\text{OCl}^-$					
13.27	3.30	6.67	3.54	1.07	0.161
13.00	3.25	8.00	3.19	0.983	0.123
12.89	3.23	8.70	3.17	0.982	0.113
12.74	3.22	9.09	3.17	0.985	0.108
12.57	3.21	9.52	3.16	0.984	0.103
12.42	3.25	8.00	3.14	0.965	0.121
12.20	3.23	8.70	3.14	0.971	0.112
11.86	3.24	8.33	3.16	0.975	0.117
11.33	3.30	6.67	3.46	1.05	0.157
10.90	3.25	8.00	3.90	1.20	0.150
10.29	3.24	8.33	7.62	2.35	0.282
10.06	3.22	9.09	17.5	5.43	0.597

<sup>a</sup>  $k_{\text{Cl}}$  and  $k_{\text{Ox}}$  have units of  $\text{M}^{-1} \text{s}^{-1} \times 10^8$ .  $[\text{OCl}^-]_0 = 1.64 \text{ M}$  (commercial) and  $[\text{OCl}^-]_0 = 2.15 \text{ M}$  (lab-prepared) at 25 °C.

**Rate of  $\text{ClO}_3^-$  and  $\text{O}_2$  formation.** In all  $\text{OCl}^-$  decomposition experiments, a downward trend in the mass balance with time occurs as calculated by means of eqs 3 and 4. For 60%  $\text{OCl}^-$  decomposition with  $[\text{OCl}^-]_0 = 2.15 \text{ M}$  and  $[\text{OH}^-]_0 = 0.126 \text{ M}$ , the mass balance decreased from 2.169–2.092 M. This is due to the visibly observable formation of oxygen during the decomposition, which is consistent with Lister.<sup>15</sup>

Plots of  $\text{OCl}^-$  decomposition as a function of  $\text{ClO}_3^-$  formed for the  $\text{OH}^-$  concentration range studied have slopes equal to  $3.23 \pm 0.04$ . If the only pathway for  $\text{OCl}^-$  decomposition is  $\text{ClO}_3^-$  formation, the slope would be 3.00 as described by the following stoichiometry for  $\text{ClO}_3^-$  formation:



The slope ( $[\text{OCl}^-]/[\text{ClO}_3^-]$ ) was not found to vary with reaction time because the  $\text{ClO}_2^-$  concentration is never more than 0.6% of the  $\text{OCl}^-$  concentration. The amount of  $\text{ClO}_2^-$  produced/consumed during the decomposition has no observable effect on the stoichiometry determination. The slopes are greater than 3 and demonstrate that  $\text{O}_2$  is formed by a minor pathway that affects the  $\text{OCl}^-/\text{ClO}_3^-$  stoichiometry, which is consistent with Lister.<sup>15</sup>



The rate expression for each decomposition pathway is:

$$d[\text{ClO}_3^-]/dt = k_{\text{Cl}}[\text{OCl}^-]^2 \quad (16)$$

$$d[\text{O}_2]/dt = k_{\text{Ox}}[\text{OCl}^-]^2 \quad (17)$$

The following relationships are used to calculate the rate constants of the two pathways:

$$\text{plot } 1/[\text{OCl}^-]_t \text{ vs time} \quad \text{slope} = 3k_{\text{Cl}} + 2k_{\text{Ox}} = k_2$$

$$\text{plot } \Delta[\text{OCl}^-] \text{ vs } [\text{ClO}_3^-] \quad \text{slope} = 3 + 2(k_{\text{Ox}}/k_{\text{Cl}})$$

The oxygen formation has measured and fitted values for  $k_{\text{Ox}}$  of  $8.9 \times 10^{-10}$  and  $5.1 \pm 0.7 \times 10^{-10} \text{ M}^{-1} \text{ s}^{-1}$ , respectively. Although the value of  $k_{\text{Ox}}$  is small and the error is large, the oxygen pathway cannot be neglected.

The rate constants for  $\text{OCl}^-$  decomposition and the rate constants for  $\text{ClO}_3^-$  and  $\text{O}_2$  formation are given in Table 5. In Table 5, the measured rate constants from second-order plots ( $3k_{\text{Cl}} + 2k_{\text{Ox}}$ ) in the 0.007–0.126 M  $\text{OH}^-$  concentration range form a minimum when compared to the results at other  $\text{OH}^-$  concentrations. This produces a minimum for the rate constants for  $\text{ClO}_3^-$  formation and  $\text{O}_2$  formation. The significant difference in the measured second-order rate constants in Table 5 for laboratory-prepared and commercial  $\text{OCl}^-$  is due to the differences in the ionic strengths as predicted by eq 8. The measured  $\text{OCl}^-/\text{ClO}_3^-$  stoichiometry is very similar for laboratory prepared and commercial  $\text{OCl}^-$ . The standard deviation of the measured slopes (0.04) is equivalent to the combined experimental error of 1.5% for the determination of the slope. The measured  $\text{OCl}^-/\text{ClO}_3^-$  stoichiometry does not vary significantly between pH 9.6 and 14. The  $\text{OCl}^-/\text{ClO}_3^-$  stoichiometry is independent of temperature,  $\text{OCl}^-$  concentration, and ionic strength. Using the average stoichiometry of  $3.23 \pm 0.04$ , the ratio of the rate constants for the two decomposition pathways ( $k_{\text{Cl}}/k_{\text{Ox}}$ ) is  $8.7 \pm 2$ .

**Acknowledgment.** The authors appreciate funding by the American Water Works Research Foundation.

**Supporting Information Available:** The concentration of  $\text{OCl}^-$ ,  $\text{ClO}_3^-$ ,  $\text{ClO}_2^-$ , measured as a function of time and the chlorine mass balance determined via eqs 3 and 4, is available for eight experiments from pH 9.60 to an  $\text{OH}^-$  concentration of 1.0 M at 25 °C with an initial concentration of 2.15 M laboratory-prepared  $\text{OCl}^-$ . This material is available free of charge via the Internet at <http://pubs.acs.org>.

IC980020Q